JBC RESEARCH ARTICLE

Non-transcriptional IRF7 interacts with NF-κB to inhibit viral inflammation

Received for publication, August 28, 2023, and in revised form, February 23, 2024 Published, Papers in Press, March 18, 2024,
https://doi.org/10.1016/j.jbc.2024.107200

Shumin Fan[1], **Sonam Popli**[1], **Sukanya Chakravarty**[1,2], **Ritu Chakravarti**[3], **and Saurabh Chattopadhyay**[1,2,*]

From the [1]*Department of Medical Microbiology and Immunology, University of Toledo College of Medicine and Life Science, Toledo, Ohio, USA;* [2]*Department of Microbiology, Immunology and Molecular Genetics, University of Kentucky College of Medicine, Lexington, Kentucky, USA;* [3]*Department of Physiology and Pharmacology, University of Toledo College of Medicine and Life Science, Toledo, Ohio, USA*

Reviewed by members of the JBC Editorial Board. Edited by Karin Musier-Forsyth

Interferon (IFN) regulatory factors (IRF) are key transcription factors in cellular antiviral responses. IRF7, a virus-inducible IRF, expressed primarily in myeloid cells, is required for transcriptional induction of interferon α and antiviral genes. IRF7 is activated by virus-induced phosphorylation in the cytoplasm, leading to its translocation to the nucleus for transcriptional activity. Here, we revealed a nontranscriptional activity of IRF7 contributing to its antiviral functions. IRF7 interacted with the pro-inflammatory transcription factor NF-κB-p65 and inhibited the induction of inflammatory target genes. Using knockdown, knockout, and overexpression strategies, we demonstrated that IRF7 inhibited NF-κB–dependent inflammatory target genes, induced by virus infection or toll-like receptor stimulation. A mutant IRF7, defective in transcriptional activity, interacted with NF-κB-p65 and suppressed NF-κB–induced gene expression. A single-action IRF7 mutant, active in anti-inflammatory function, but defective in transcriptional activity, efficiently suppressed Sendai virus and murine hepatitis virus replication. We, therefore, uncovered an anti-inflammatory function for IRF7, independent of transcriptional activity, contributing to the antiviral response of IRF7.

The innate immune response is the first line of defense against virus infections. Production of type-I interferons (IFNs) is indispensable for establishing innate immune responses and plays a significant role in establishing adaptive immune responses in virus infections (1–5). Two best-known type-I IFNs are IFNα and IFNβ; while most cells can produce IFNβ, hematopoietic cells are primary producers of IFNα (6–8). Upon infections, virus components such as viral RNAs are recognized by pathogen recognition receptors (PRR) of host cells. For example, the retinoic acid-inducible gene I, located in the cytosol, and toll-like receptors (TLRs), such as TLR3 on endosomal membrane, recognize foreign RNAs. PRRs are essential in recognizing RNA viruses upon infection; once PRRs bind viral components, they transduce signals to activate downstream pathways for type-I IFN production. One family of such key molecules is IFN regulatory factors (IRFs), among which IRF3 and IRF7 are essential for type-I IFN production (1, 9). IRF3 and IRF7 are activated by phosphorylation and translocate into the nucleus to act as transcription factors for induction of type-I IFNs. Type-I IFNs are then secreted and bind to their cognate receptors, for example, IFNARs, to activate JAK/STAT-dependent signaling pathways to induce a variety of genes known as IFN-stimulated genes (ISGs). Many ISGs encode proteins that possess antiviral properties and protect the host from virus infections (4, 10–12). Efficient viral replications in primary target organs or systemic spread of virus particles could cause direct damage to the host when host defense mechanisms fail, for example, in case of delayed IFN responses (13). For example, HIV-1 could establish persistent infection in humans by impairing the host type-I IFNs responses (14).

In addition to type-I IFNs, virus infection also activates NF-κB pathways, leading to induction of pro-inflammatory cytokines. NF-κB is a key regulator of inflammation, and it consists of five family members (p65, RelB, cRel, p50, and p52) that form dimers. Dimeric NF-κB binds to DNA to act as transcription factor for inflammatory gene expressions (15, 16). While inflammation is required for host defense in early stage of virus infection, aberrant inflammatory responses could harm the host. In fact, many viruses can hijack host's inflammatory response system to their benefit while causing damage to the host (17). For example, human cytomegalovirus encodes agonists of NF-κB to activate inflammation that facilitates the virus reactivation and entry to lytic replication cycle in host cells (18). In Influenza A virus (IAV) infection, excessive inflammation plays a major role in pathogenesis, such as lung damage (19, 20). For newly emerged SARS-CoV-2, which causes COVID-19, patients suffered severe complications such as multi-organ failure, systemic shock, etc., due to cytokine storm led by unchecked NF-κB pathway overproducing pro-inflammatory cytokines (21). Therefore, in addition to virus replication, dysregulated host immune responses, such as overacting inflammatory response, could be a culprit of pathogenesis and lead to increased morbidity and mortality upon virus infections. It is, therefore, critical to better

* For correspondence: Saurabh Chattopadhyay, Saurabh.Chattopadhyay@uky.edu.

understand the mechanisms by which virus-induced inflammation is regulated.

IRF7 is the "master regulator" of type-I IFN in innate antiviral responses (22). IRF7 deficiency leads to enhanced susceptibility to severe IAV infection in mice and humans due to impaired type-I IFNs production (23–25). Recent studies revealed that individuals with defective IRF7 functions are more vulnerable to severe COVID-19 (26, 27). Distinct from its close family member IRF3, IRF7 is predominantly expressed in immune cells such as pDCs and monocytes, and its expression is inducible in various cell types upon stimuli such as virus infections (23). While IRF7 acts as a key transcription factor for type-I IFNs (particularly IFNα), it is also an ISG, becoming an important mediator in the feedback loop for type-I IFN amplification (28). IRF7 is critical in establishing a positive feedback loop for late phase type-I IFN and other antiviral factors amplification against IAV infection in human lung epithelium (29). Although IRF7 regulates oncogenesis, cell differentiation, and apoptosis, these functions have not been fully elucidated (30).

IRF7 and NF-κB are two major transcription factors activated during viral infection. However, their interaction and impact on regulating inflammation have not been well understood (31, 32). Previous studies demonstrated the potential of IRFs to crosstalk with other signaling pathways in preventing excessive inflammatory responses in virus infection (32–35). Our recent study demonstrated that IRF3 plays an anti-inflammatory role in virus infections by interacting with NF-κB-p65 subunit (36, 37). IRF3 interacts with NF-κB-p65 subunit directly in the cytosol *via* specific binding motifs on both proteins. As a result of this interaction, IRF3 inhibits the activation of NF-κB-p65 and its induced inflammatory target genes. IRF3 KO mice, upon infection, also resulted in increased inflammatory genes, which likely contribute to viral pathogenesis. In this study, we identified a motif in IRF7 similar to the NF-κB-p65–binding site of IRF3. As a result, IRF7 also interacted with NF-κB-p65 subunit and subsequently, suppressed NF-κB–dependent inflammatory gene expression. Furthermore, the anti-inflammatory function of IRF7 also contributed to its antiviral functions.

Results

IRF7 possesses NF-κB–binding motif of IRF3 and interacts with NF-κB-p65

Recently, we uncovered a new function of IRF3, inhibiting virus-induced inflammatory gene expression (36, 37). For anti-inflammatory function, IRF3 interacts with NF-κB-p65 subunit via specific domains and inhibits its nuclear translocation (36). Here, we further reveal, using co-immunoprecipitation (co-IP) assay, IRF3 interacted with NF-κB-p65 but not NF-κB-p50 subunit (Fig. 1*A*). These results indicate an affinity of IRF3 for p65 but not p50 subunit of NF-κB. Our previous studies identified an NF-κB-p65–binding motif in IRF3 (36). We inquired whether other IRFs possess a similar motif and performed bioinformatic analyses of NF-κB-p65–interacting IRF3 motif in other IRFs. Sequence alignment analyses revealed that IRF5 and IRF7 also contained NF-κB-p65–interacting IRF3 protein sequence (Fig. 1*B*). Using this lead, we performed co-IP analyses to validate bioinformatic results; similar to IRF3, IRF5 and IRF7 also interacted with NF-κB-p65 (Fig. 1*C*). We pursued IRF7, which is activated by mechanisms similar to IRF3 and is a key regulator of antiviral responses. We further evaluated the specificity of IRF7 interaction; our results indicated IRF7, like IRF3, also interacted with p65 but not p50 subunit of NF-κB (Fig. 1*D*). We validated our co-IP results by proximity ligation assay (PLA), which confirmed IRF7:NF-κB-p65 interaction (Fig. 1*E*). Encouraged by biochemical and bioinformatic results, we performed secondary structure alignment and revealed both human and mouse IRF7 proteins contained IRF3-like NF-κB–binding motifs (Fig. 1*F*). Therefore, IRF7 possesses NF-κB–binding motif and interacted with p65 subunit.

IRF7 interacts with NF-κB-p65 independent of its transcriptional activation

We inquired whether IRF7 required its transcriptional activation to interact with NF-κB. For transcriptional activation, IRF7 is phosphorylated on Ser^{425} and Ser^{426} in the C-terminal domain (Fig. 2*A*, (38)). Mutating these Ser residues to Ala inhibits IRF7 transcriptional activation and IRF7-dependent gene induction (38). We engineered a mutant, IRF7-S1 ($IRF7^{SS425/26AA}$), which is defective in these phosphorylation sites (Fig. 2*A*), and tested its functions. To this end, we generated IRF3 KO HEK293T cells, to avoid any contribution of IRF3, using CRISPR/Cas9 system and expressed IRF7-Wt or IRF7-S1 at similar protein levels (Fig. 2*B*). IRF7-Wt was robustly phosphorylated by Sendai virus (SeV) infection; however, IRF7-S1 mutant, as expected, remained unphosphorylated (Fig. 2*C*). We validated IRF7-S1 was transcriptionally inactive by testing SeV-induced IFIT3, an IRF-dependent gene, at mRNA (Fig. 2*D*) and protein (Fig. 2*E*) levels. These results confirmed IRF7-S1 mutant was defective in phosphorylation and transcriptional activity in our cellular model. Moreover, IRF7 could functionally compensate for IRF3 to induce IFIT3 gene. We evaluated whether IRF7-S1 interacted with NF-κB-p65; co-IP results indicated both Wt and S1 proteins interacted with NF-κB-p65 with similar affinities (Fig. 2*F*). We further validated the interaction of IRF7-S1 with p65 using PLA (Fig. 2*G*). These results demonstrated IRF7 interacted with NF-κB-p65 independent of its phosphorylation and transcriptional activation. We further inquired whether p-IRF7 interacts with p65 and performed co-IP assay, which indicated that p-IRF7 was able to interact with p65 (Fig. 2*H*). Therefore, although p-IRF7 interacted with p65, phosphorylation of IRF7 was not a prerequisite for the interaction.

To test whether IRF7:p65 interaction was direct, we isolated epitope-tagged IRF7 and p65 proteins, in near purity, from SeV-infected cells and set up cell-free interaction assay (Fig. S1). Cell-free interaction, followed by co-IP analyses, indicated that IRF7 and p65 proteins bound directly, without any conduit protein (Fig. 3*A*). Direct IRF7:p65 interaction led us to map interacting domains between the two proteins. We designed a series of C-terminally deleted mutants of IRF7 (Fig. 3*B*) and NF-κB-p65 (Fig. 3*C*) and examined their

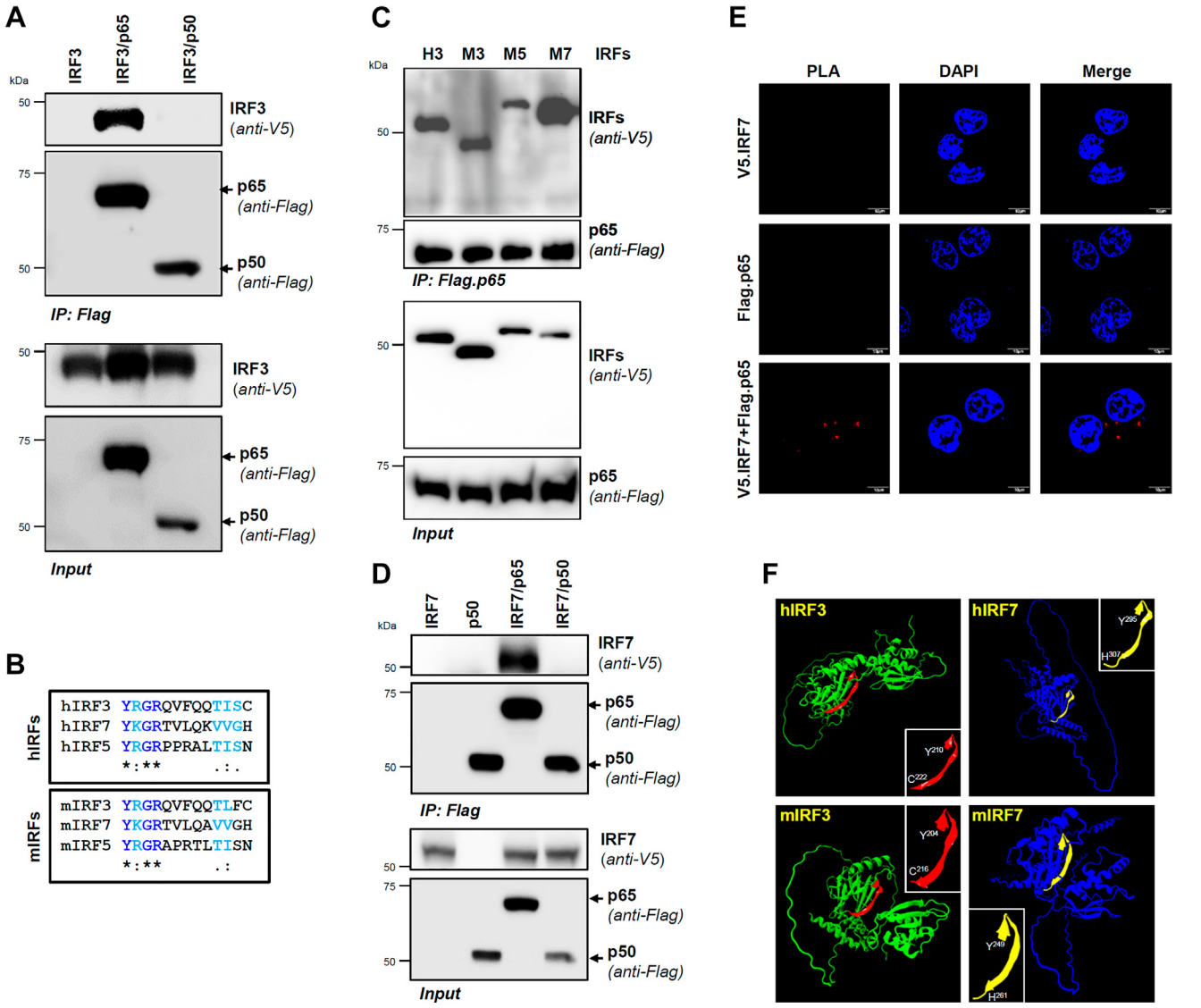

Figure 1. IRF7 interacts with NF-κB-p65 subunit. *A*, HEK293T cells were co-transfected with V5.IRF3 and Flag.p65 or Flag.p50, as indicated, and infected with SeV for 2 h, and subjected to co-immunoprecipitation analyses. *B*, the NF-κB–interacting IRF3 peptide sequence was used for alignment analyses for human and mouse IRFs, as indicated. *, fully conserved amino acids, moderately conserved amino acids, weakly conserved amino acids. *C*, HEK293T cells were co-transfected with V5.IRFs (as indicated, H, human and M, mouse) and Flag.p65, infected with SeV for 2 h, and subjected to co-immunoprecipitation analyses. *D*, HEK293T cells were co-transfected with V5.IRF7 and Flag.p65 or Flag.p50, as indicated, and infected with SeV for 2 h, and subjected to co-immunoprecipitation analyses. *E*, HEK293T cells, co-transfected with V5.IRF7 and Flag.NF-κB-p65, were infected with SeV and immunostained with anti-Flag and anti-V5 antibodies and analyzed by proximity ligation assay; scale bar represents 10 μm. *F*, the NF-κB–interacting IRF3 peptide was used to model the presence of such a motif in human and mouse IRF7. IRF, interferon regulatory factor; SeV, Sendai virus.

interaction using co-IP. Domain mapping analyses revealed IRF7 domain 237-410 was required for interaction with NF-κB-p65 (Fig. 3*D*), and NF-κB-p65 domain 426-443 was required for IRF7 interaction (Fig. 3*E*). We further validated these results using critical deletion mutants of both proteins (Fig. 3*F*). These results demonstrated IRF7 and p65 interacted directly using specific domains to form a complex.

IRF7 interaction inhibits phosphorylation and nuclear translocation of NF-κB-p65

To investigate the interaction of IRF7 and p65 more closely, we used endogenous proteins, viral and non-viral inducers, and kinetics of interaction. Epitope-tagged IRF7 interacted, time-dependently, with p65, upon SeV infection (Fig. 4*A*) or polyI:C stimulation (TLR3, Fig. 4*B*). IRF7:p65 complex was cytosolic, indicated earlier using IRF7-S1 mutant, which is cytosolic, and was further confirmed using cellular fractionation. Cytosolic but not nuclear IRF7 interacted with p65 (Fig. 4*C*). Next, we used endogenous IRF7 and p65 proteins and confirmed their interaction in SeV-infected cells, using co-IP (Fig. 4*D*) and PLA (Fig. 4*E*). To test the immediate effects of IRF7:p65 interaction, we investigated activation of p65 in IRF7-KD RAW264.7 cells, generated by stable expression of IRF7-specific shRNA. SeV infection caused rapid activation of p65, analyzed by its phosphorylation in control cells [RAW264.7 cells expressing non-targeting (NT) shRNA, Fig. 4*F*]. Phosphorylation of p65 was enhanced in IRF7-KD cells, indicating that reduced expression of IRF7 led to

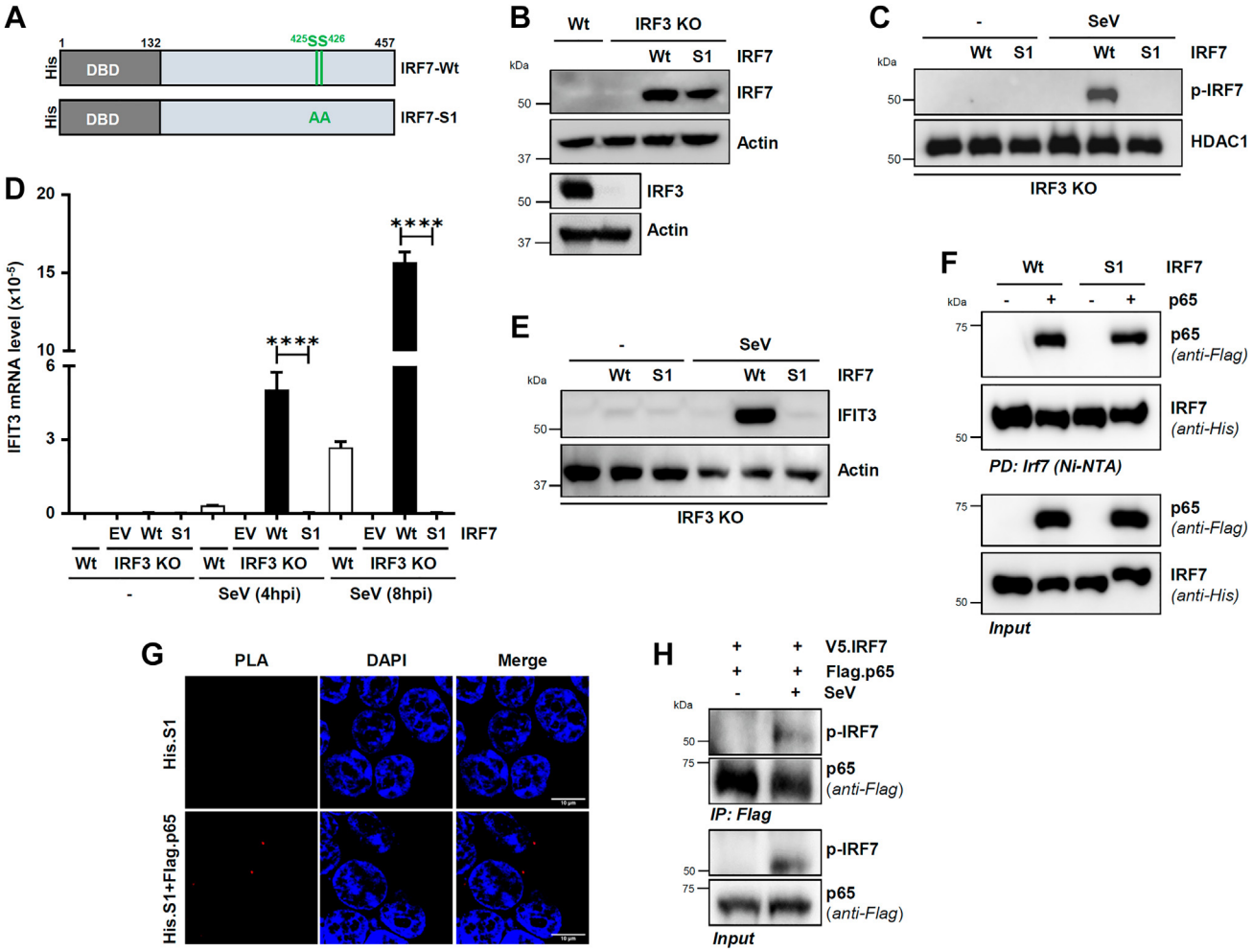

Figure 2. Transcriptional activation of IRF7 is not required for its interaction with NF-κB. *A*, a diagram showing murine IRF7 - Wt and the transcriptionally-inactive S1 mutant. *B–E*, IRF3 KO HEK293T cells, expressing IRF7-Wt or IRF7-S1, were analyzed for IRF7 expression by immunoblot (*B*), or infected with SeV, and analyzed for phosphorylated IRF7 in nuclear fractions by immunoblot (*C*), IFIT3 mRNA levels at the indicated time post-infection by qRT-PCR (*D*), or IFIT3 protein levels by immunoblot (*E*). *F*, HEK293T cells were cotransfected with His.IRF7-Wt or His.IRF7-S1 and Flag.p65, infected with SeV, and the cell lysates were pulled down using Ni-NTA beads and subjected to immunoblot for p65. *G*, HEK293T cells, co-transfected with His.IRF7-S1 and Flag.NF-κB-p65, as indicated, were infected with SeV and immunostained with anti-Flag and anti-His antibodies and analyzed by proximity ligation assay; scale bar represents 10 μm. *H*, HEK293T cells, co-transfected with V5.IRF7 and Flag.NF-κB-p65, as indicated, and were infected with SeV for 4 h when co-immunoprecipitation analyses were performed. The data represent mean ± SEM (D), **** $p < 0.0001$. DBD, DNA-binding domain; IRF, interferon regulatory factor; SeV, Sendai virus.

increased activation of p65 (Fig. 4*F*). Phosphorylation of p65 leads to its nuclear translocation and we tested whether IRF7 also inhibits this step. Indeed, IRF7-KD cells displayed increased translocation of p65 to nucleus, compared to the control cells (Fig. 4*G*). Together, these results demonstrated IRF7:p65 interaction led to the inhibition of p65 activation and its translocation to the nucleus.

IRF7 inhibits NF-κB–induced inflammatory gene expression

To investigate whether IRF7:NF-κB-p65 binding leads to inhibition of NF-κB–induced genes, we ectopically expressed IRF7 in HT1080 human cell line, a robust inducer of inflammatory and antiviral genes. IRF7 expression significantly inhibited TNFAIP3/A20 induction by SeV infection (Fig. 5*A*). Similar to SeV infection, upon RLR stimulation by cytosolic polyI:C, TNFAIP3/A20 protein induction was also strongly inhibited in IRF7-expressing cells (Fig. 5*B*). We further examined TNFAIP3 mRNA induction; IRF7 expression significantly inhibited RLR-induced TNFAIP3 mRNA induction (Fig. 5*C*). We validated these findings in Let1 mouse lung epithelial cell line, where we stably expressed IRF7 (Fig. 5*D*). IRF7 expression, as expected, increased Ifnb1 gene induction (Fig. 5*E*), which requires IRF transcriptional activity upon RLR stimulation. However, IRF7 expression, expectedly, inhibited Tnfaip3 gene induction upon RLR stimulation (Fig. 5*F*). We further examined whether IRF7 could suppress elevated NF-κB–induced gene expression, caused by IRF3 deficiency. Indeed, ectopic expression of either IRF3 or IRF7 efficiently suppressed elevated A20 induction in IRF3 KO HT1080 cells (Fig. 5*G*).

We examined whether IRF7 underexpression leads to increased NF-κB–induced gene expression. To test this, we used Let1 cell line, in which SeV infection caused robust

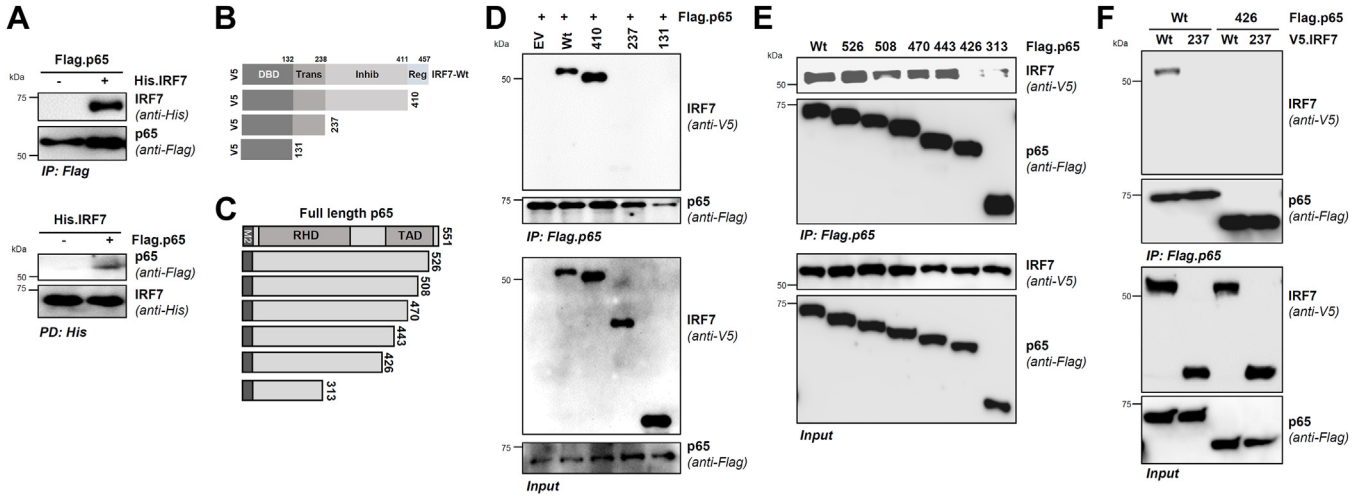

Figure 3. Domain mapping of IRF7:NF-κB-p65 interaction. *A*, Flag.p65 or His.IRF7 proteins were isolated using the method shown in Figure S1, and subjected to cell-free interaction, followed by co-immunoprecipitation analyses. *B* and *C*, V5.IRF7 and its deletion mutants and Flag.p65 and its deletion mutants used for the interaction studies. *D*, HEK293T cells were co-transfected with Flag.p65 and V5.IRF7 (Wt or deletion mutants, as shown), infected with SeV, and analyzed by co-immunoprecipitation. *E*, HEK293T cells were co-transfected with V5.IRF7 and Flag.p65 (Wt or deletion mutants, as indicated), infected with SeV, and analyzed by co-immunoprecipitation. *F*, HEK293T cells were co-transfected with Flag.p65 and V5.IRF7, (Wt or deletion mutants, as indicated), infected with SeV, and analyzed by co-immunoprecipitation. EV, empty vector; IRF, interferon regulatory factor; SeV, Sendai virus.

induction of IRF7 mRNA in NT shRNA (shNT)-expressing cells but not in IRF7-shRNA (shIRF7)-expressing cells (Fig. 6*A*). SeV infection, as expected, caused robust Ifit3 induction in shNT cells but not in shIRF7 cells (Fig. 6*B*). Similar to SeV infection, RLR stimulation also induced IRF7 in shNT but not in shIRF7 cells (Fig. 6*C*). Induction of IRF7-target genes, Ifna and Ifnb1, as expected, were suppressed in IRF7-KD cells (Fig. 6, *D* and *E*). RLR-induced inflammatory genes,

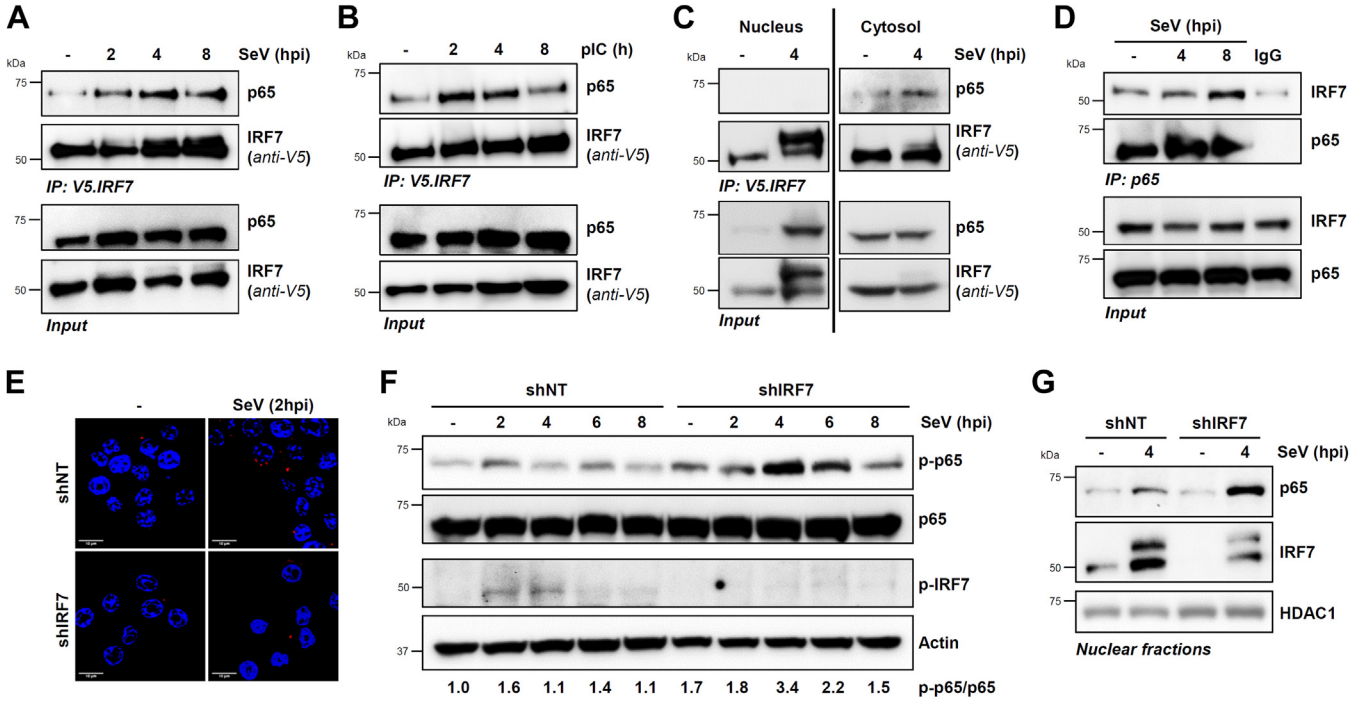

Figure 4. Endogenous IRF7 interacts with NF-κB-p65 and interferes with its transcriptional activation. *A*, IRF3 KO HT1080 cells expressing V5.IRF7 were infected with SeV for the indicated time, when co-immunoprecipitation analyses were performed, as indicated. *B*, IRF3 KO HT1080 cells expressing V5.IRF7 were treated with polyI:C (pIC) to activate TLR3 signaling for the indicated time, when co-immunoprecipitation analyses were performed, as indicated. *C*, IRF3 KO HT1080 cells expressing V5.IRF7 were infected with SeV for the indicated time, when co-immunoprecipitation analyses were performed from nuclear and cytosolic fractions, as indicated. *D*, Let1 cells were infected with SeV for the indicated time, when co-immunoprecipitation analyses were performed using endogenous IRF7 and NF-κB-p65 proteins. *E*, RAW264.7 cells, lentivirally expressing non-targeting (NT) or IRF7-specific shRNA, were infected with SeV, and endogenous IRF7 and p65 proteins were immunostained and analyzed by proximity ligation assay; scale bar represents 10 μm. *F*, RAW264.7 cells, lentivirally expressing NT or IRF7-specific shRNA, were infected with SeV for the indicated time and analyzed for p-p65, p65, p-IRF7 by immunoblot. Image J analyses of p-p65/p65 were performed and shown at the bottom of the panel. *G*, RAW264.7 cells, lentivirally expressing NT or IRF7-specific shRNA, were infected with SeV for the indicated time and the nuclear fractions were analyzed for p65 and IRF7 by immunoblot. IRF, interferon regulatory factor; SeV, Sendai virus.

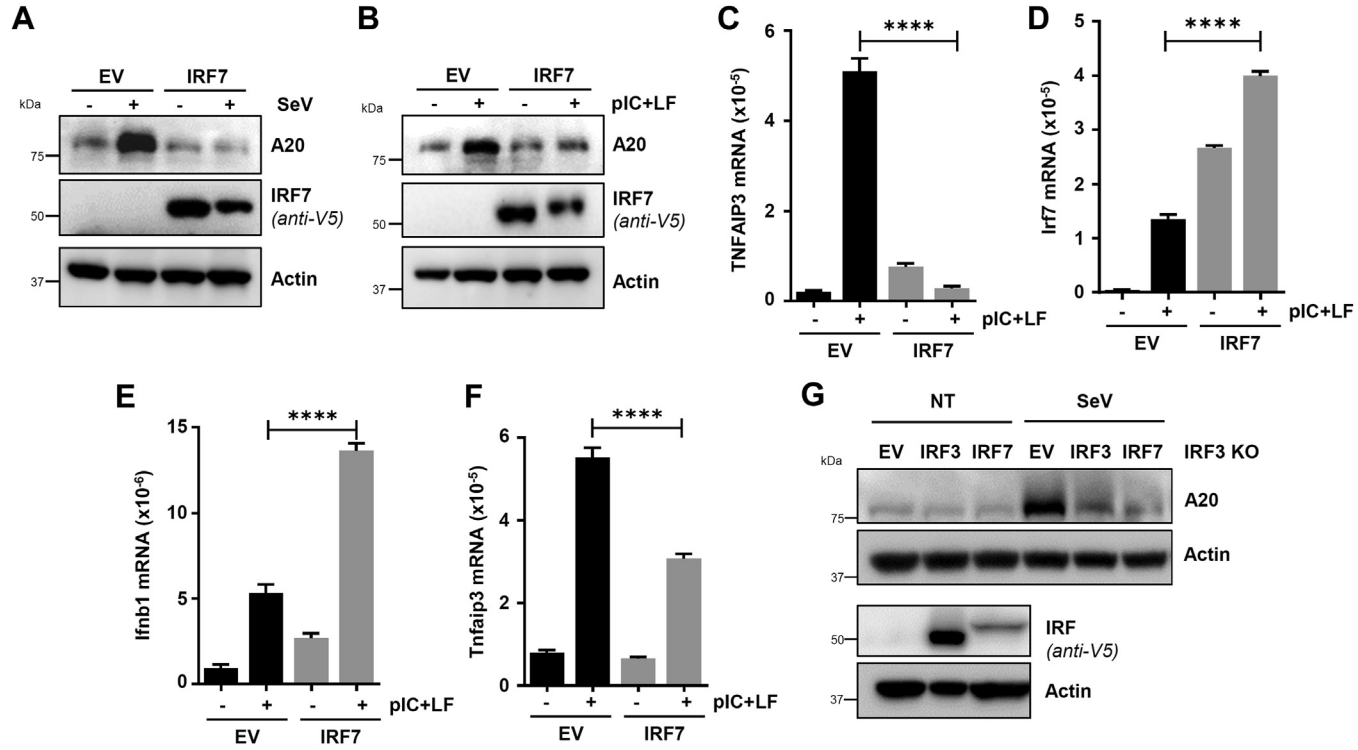

Figure 5. Ectopic expression of IRF7 inhibits inflammatory target gene expression in HT1080 and Let1 cells. *A* and *B*, HT1080 cells, ectopically expressing IRF7, were either infected with SeV (*A*) or transfected with polyI:C (pIC+LF, B) and the protein levels for A20 were analyzed by immunoblot. *C*, HT1080 cells, ectopically expressing IRF7, were transfected with polyI:C (pIC+LF) and TNFAIP3 mRNA levels were analyzed by qRT-PCR. *D–F*, Let1 cells, stably expressing IRF7, were left untreated (*D*) or transfected with polyI:C (pIC+LF) for 4 h (*E*, *F*), when the mRNA levels for Irf7, Ifnb1, and Tnfaip3 were analyzed by qRT-PCR. *G*, IRF3 KO HT1080 cells were ectopically transfected with IRF3 or IRF7, as indicated, and infected with SeV for 8 h, when the cell lysates were analyzed for A20 and IRF by immunoblot. The data represent mean ± SEM (C-F), **** $p < 0.0001$. EV, empty vector; IRF, interferon regulatory factor; LF, Lipofectamine 2000; SeV, Sendai virus.

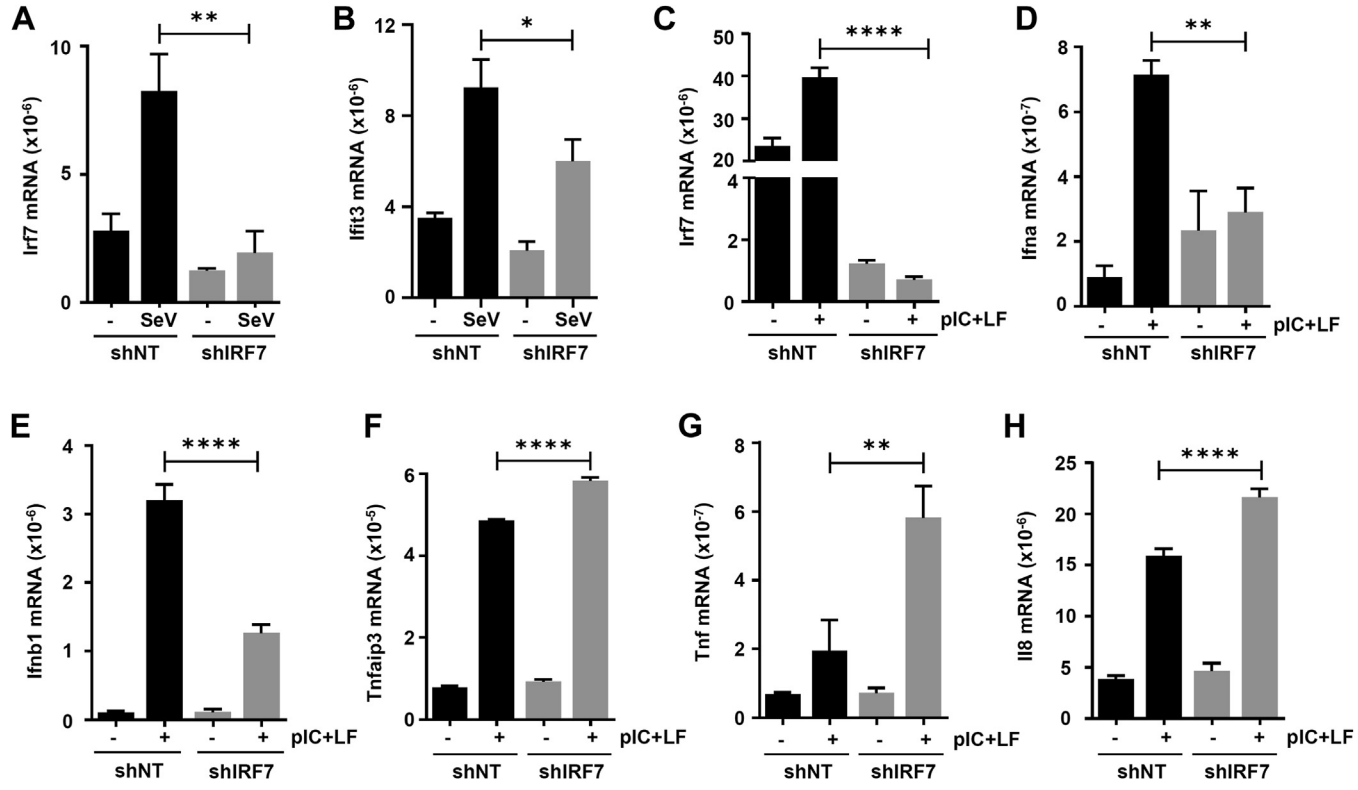

Figure 6. IRF7 knockdown mouse lung epithelial cells exhibit increased inflammatory gene induction in response to virus infection or RLR signaling. *A–H*, Let1 cells, lentivirally expressing non-targeting (NT) or IRF7-specific shRNA, were either infected with SeV (8 h, *A*, *B*) or transfected with polyI:C (pIC+LF, 4 h, *C–H*), when the mRNA levels of Irf7, Ifit3, Ifna, Ifnb1, Tnfaip3, Tnf, and Il8 were analyzed by qRT-PCR. The data represent mean ± SEM, * $p < 0.05$, ** $p < 0.01$, **** $p < 0.0001$. IRF, interferon regulatory factor; SeV, Sendai virus.

for example, Tnfaip3, Tnf, and Il8, were significantly elevated (Fig. 6, *F–H*). Next, we used myeloid cells, RAW264.7 macrophage cell line, and IRF7 KO immortalized bone marrow-derived macrophages, to test IRF7-mediated suppression of NF-κB–induced genes. In IRF7-KD RAW264.7 cells (Fig. 7*A*), murine hepatitis virus (MHV)-induced Tnfaip3 gene expression was elevated compared to the control cells (Fig. 7*B*). We used a strong activator of NF-κB, lipopolysaccharide (LPS), which like other activators, also elevated NF-κB–induced genes (Tnfaip3 and Tnf) in IRF7-KD cells (Fig. 7, *C* and *D*). Similar to RAW264.7 cell line, IRF7 KO iBMDMs also expressed elevated NF-κB–induced genes (Tnfaip3 and Tnf) upon LPS stimulation (Fig. 7, *E–G*). Therefore, IRF7 suppressed NF-κB–induced genes in myeloid and non-myeloid cell types.

IRF7 inhibits virus replication in myeloid and non-myeloid cells

We recently reported a new antiviral function of IRF3 by inhibiting NF-κB activation and the induced genes (36, 37). Since IRF7 regulates NF-κB–induced genes, we evaluated whether this function contributes to antiviral activities of IRF7. In Let1 cells, IRF7 KD led to increased IAV (Fig. 8*A*), SeV (Fig. 8*B*), and MHV (Fig. 8*C*) viral mRNA levels, indicating the ability of IRF7 in mediating antiviral functions in epithelial cells. We further expanded the antiviral activities of IRF7 to myeloid cells, which are primary responders of IRF7 functions (23, 28). TLR4 stimulation by LPS (Fig. 8*D*) or retinoic acid-inducible gene I stimulation by SeV infection (Fig. 8*E*) robustly induced IRF7 mRNA in Wt but not IRF7 KO iBMDMs. We evaluated antiviral gene expression in iBMDMs; SeV infection, as expected, robustly induced Ifnb1 (Fig. 8*F*) and Ifit1 (Fig. 8*G*) genes in Wt but not IRF7 KO iBMDMs (Fig. 8, *F* and *G*). Subsequently, SeV replication was enhanced in IRF7 KO iBMDMs compared to Wt cells (Fig. 8*H*). Similar to SeV, IRF7 was strongly induced by MHV (Fig. 8*I*), and IRF7 KO iBMDMs displayed elevated MHV viral mRNA levels compared to Wt cells (Fig. 8*J*). Elevated viral gene expression led to increased infectious virus particle release from IRF7 KO cells, compared to Wt cells, analyzed at various times post infection (Fig. 8*K*). IRF7, therefore, was required for antiviral gene expression and inhibition of virus replication in both myeloid and non-myeloid cells.

Transcriptionally inactive IRF7 inhibits NF-kB activity and viral replication

IRF7 interacted with NF-κB-p65 independent of its phosphorylation and transcriptional activation (Fig. 2, *F* and *G*). We evaluated whether nontranscriptional IRF7 mutant can suppress NF-κB activity and viral replication. To address this, we

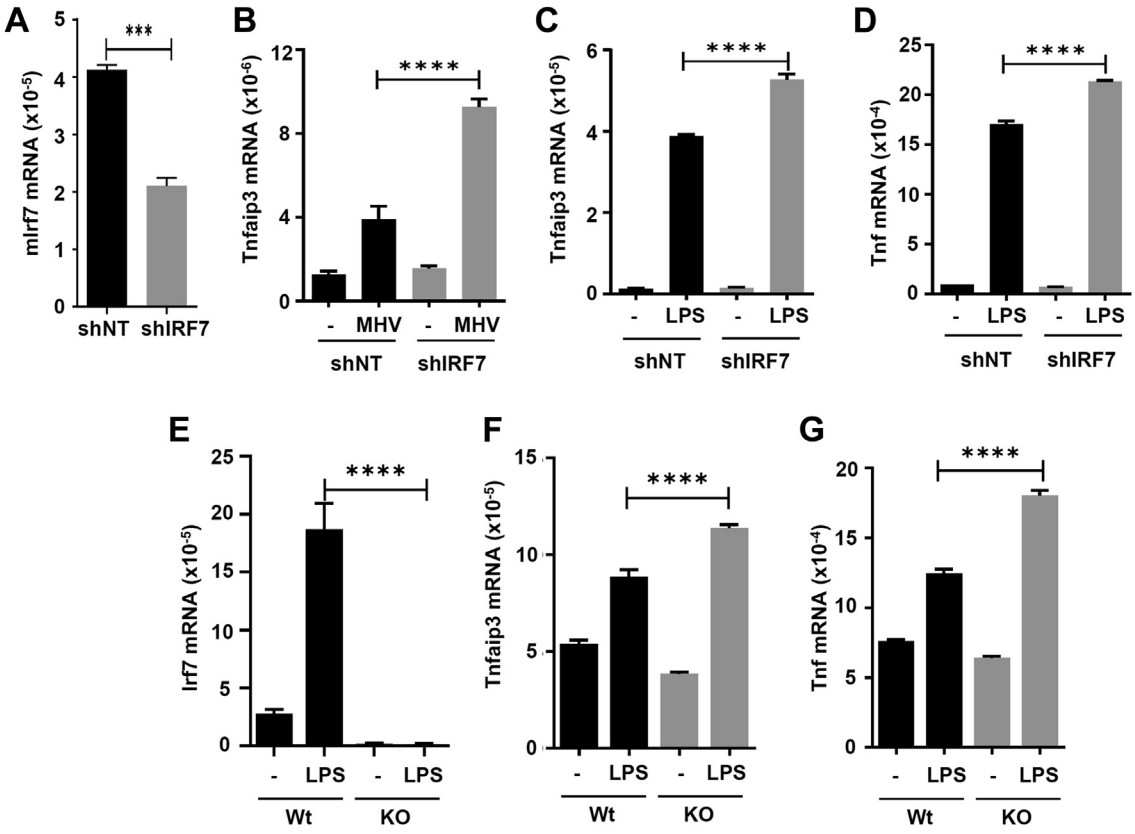

Figure 7. IRF7 knockdown or knockout in macrophages increased inflammatory gene induction in response to virus infection or TLR signaling. *A–D*, RAW264.7 cells, lentivirally expressing non-targeting (NT) or IRF7-specific shRNA (*A*), were either infected with MHV (4 h, *B*) or treated with LPS (4 h, *C*, *D*), and the mRNA levels of Irf7, Tnfaip3, and Tnf were analyzed by qRT-PCR. *E–G*, Wt or IRF7 KO iBMDMs were either left untreated or treated with LPS (4 h), when the mRNA levels of Irf7, Tnfaip3, and Tnf, as indicated, were analyzed by qRT-PCR. The data represent mean ± SEM, *** $p < 0.001$, **** $p < 0.0001$. IRF, interferon regulatory factor; LPS, lipopolysaccharide; MHV, murine hepatitis virus.

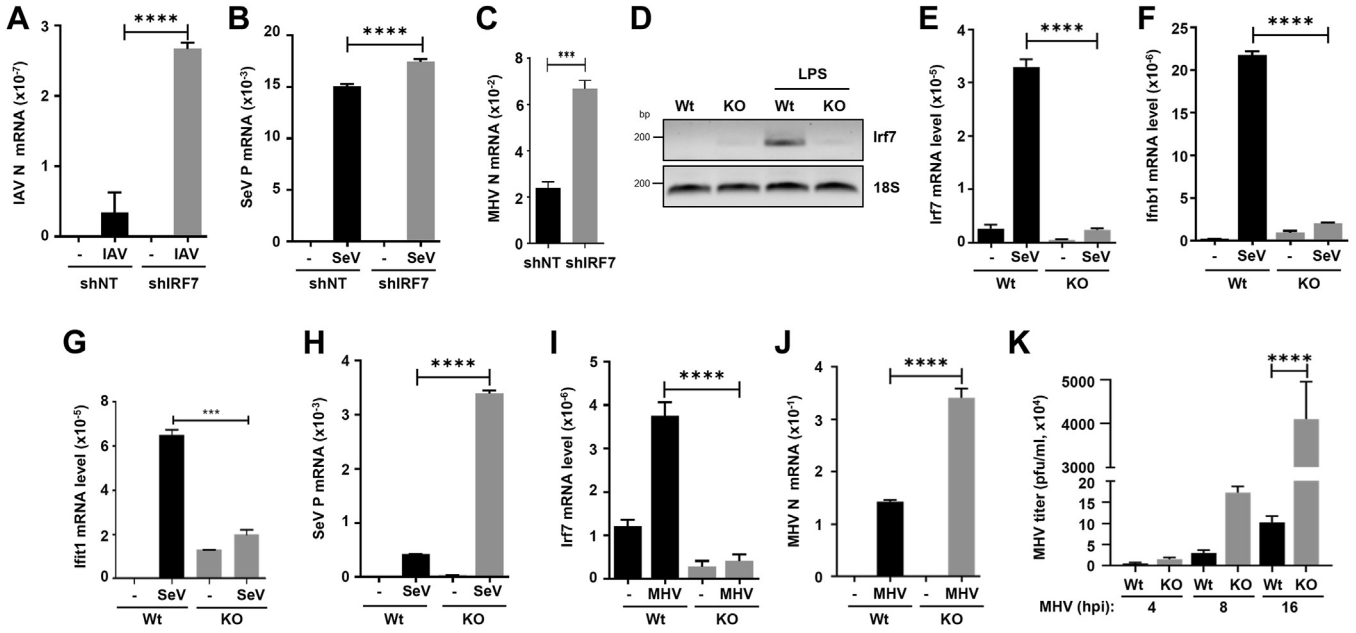

Figure 8. IRF7-deficiency leads to increased viral replication. *A–C*, Let1 cells, lentivirally expressing either non-targeting (NT) or IRF7-specific shRNA, were infected with IAV (*A*), SeV (*B*), or MHV (*C*), and the viral mRNA levels were analyzed by qRT-PCR. *D*, Wt and IRF7 KO iBMDMs were treated with LPS (1 μg/ml) and the RNA was analyzed by RT-PCR for IRF7 and 18 s rRNA. *E–H*, Wt or IRF7 KO iBMDMs were infected with SeV (4 hpi) and the cellular (Irf7, Ifnb1, Ifit1) or viral (SeV P) mRNA levels were analyzed by qRT-PCR. *I* and *J*, Wt or IRF7 KO iBMDMs were infected with MHV (4 hpi) and the cellular (Irf7) or viral (MHV N) mRNA levels were analyzed by qRT-PCR. *K*, Wt or IRF7 KO iBMDMs were infected with MHV and the infectious virus release was analyzed by plaque assay at the indicated time post-infection. The data represent mean ± SEM (A-C, E-K), *** $p < 0.001$, **** $p < 0.0001$. IAV, Influenza A virus; IRF, interferon regulatory factor; LPS, lipopolysaccharide; MHV, murine hepatitis virus; SeV, Sendai virus.

expressed IRF7-Wt or IRF7-S1 in IRF7 KO iBMDMs and tested NF-κB activity upon MHV infection. MHV infection caused increased Tnfaip3 gene induction in IRF7 KO cells (Fig. 9*A*, EV). Expression of either IRF7-Wt or IRF7-S1 significantly suppressed MHV-induced Tnfaip3 expression at various times post infection (Fig. 9*A*). Similarly, MHV-induced Il1b was suppressed by both IRF7-Wt and IRF7-S1 (Fig. S2). These results indicated IRF7-mediated suppression of NF-κB activity was independent of its transcriptional activation.

To evaluate whether IRF7 non-transcriptional mutant can confer its antiviral functions, we examined antiviral activity of IRF7-S1 mutant against MHV and SeV, which were restricted by IRF7 (Fig. 8). MHV replication, examined by viral N protein expression, was inhibited by ectopic expression of IRF7-Wt or IRF7-S1 in NIH3T3 (Fig. 9*B*) and L929 (Fig. 9*C*) cell lines, to further expand the new IRF7 functions to fibroblasts. Furthermore, MHV replication, analyzed by viral mRNA levels, was increased in IRF7 KO iBMDMs (EV) compared to Wt control at various times post infection (Fig. 9*D*). Expression of either IRF7-Wt or IRF7-S1 mutant significantly suppressed MHV replication at various times post infection (Fig. 9*D*). Subsequently, both Wt and S1 mutant of IRF7 efficiently suppressed MHV infectious particle release compared to IRF7 KO iBMDMs (Figs. 9*E* and S3). IRF7-Wt and IRF7-S1 expression also significantly suppressed SeV replication, analyzed by viral protein expression, in NIH3T3 and L929 cells (Fig. 9, *F* and *G*). We expanded antiviral functions of non-transcriptional IRF7 to human cells and used IRF3 KO HEK293T cells. In IRF3 KO HEK293T, SeV viral mRNA expression was significantly increased compared to Wt control (Fig. 9*H*). In IRF3 KO cells, expression of IRF7-Wt suppressed viral mRNA levels (Fig. 9*H*). IRF7-S1 mutant, similar to IRF7-Wt, also suppressed viral replication at different times post infection, compared to EV control (Fig. 9*H*). Together, our results demonstrated transcriptionally inactive mutant of IRF7 with anti-NF-κB activity suppressed replication of MHV and SeV in human and mouse cells.

Discussion

We report here a novel nontranscriptional function of IRF7, suppressing cellular inflammatory response and viral replication. We recently reported IRF3, a key member of the IRF family of transcription factors, inhibits NF-κB–induced genes and subsequently, suppresses viral inflammation. IRF3 performs this function independent of its activation in transcriptional or pro-apoptotic pathways. Molecular basis of this IRF3 function is its ability to interact with NF-κB-p65 subunit using specific binding motif and inhibiting its nuclear translocation. Using sequence alignment analyses, we detected a similar NF-κB–binding motif in IRF7. Based on *in silico* analyses, we performed biochemical studies and revealed that IRF7 interacted with NF-κB-p65 but not with NF-κB-p50. To investigate functional consequence of IRF7:NF-κB interaction, we examined NF-κB–dependent inflammatory gene expression in the presence or absence of IRF7. IRF7-deficient cells exhibited increased NF-κB–dependent genes compared to Wt cells. To determine whether transcriptional activation of IRF7 was required for anti-inflammatory function of IRF7, we generated IRF7-S1 mutant, defective in transcriptional

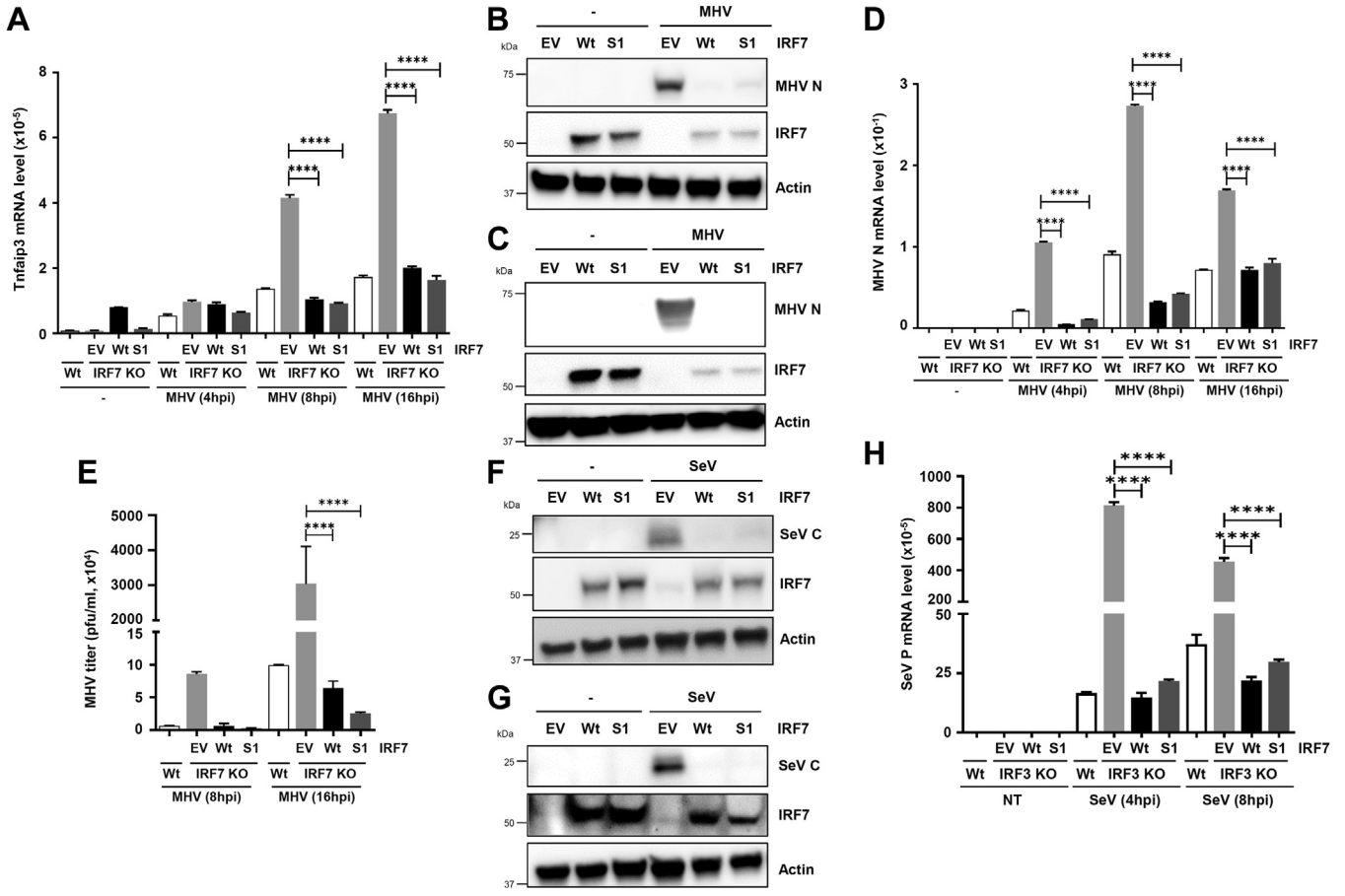

Figure 9. Transcriptionally inactive but anti-inflammatory IRF7 mutant can inhibit viral replication. *A*, IRF7 KO iBMDMs, lentivirally expressing IRF7-Wt or IRF7-S1, were infected with MHV for the indicated time and analyzed for Tnfaip3 mRNA levels by qRT-PCR. *B* and *C*, NIH3T3 (*B*) or L929 (*C*) cells were infected with MHV (MOI:5, 16hpi) and MHV N protein levels were analyzed by immunoblot. *D*, Wt or IRF7 KO iBMDMs, reconstituted with Wt or S1 mutant of IRF7, as indicated, were infected with MHV for the indicated time, when the viral mRNA levels were analyzed by qRT-PCR. *E*, Wt or IRF7 KO iBMDMs, reconstituted with Wt or S1 mutant of IRF7, as indicated, were infected with MHV for the indicated time, when the infectious virus particle release was analyzed by plaque assay. *F* and *G*, NIH3T3 (*F*) or L929 (*G*) cells were infected with SeV (MOI:5, 16hpi) and viral C protein levels were analyzed by immunoblot. *H*, Wt or IRF3 KO HEK293T cells, reconstituted with Wt or S1 mutant of IRF7, were infected with SeV for the indicated time, when the viral mRNA levels were analyzed by qRT-PCR. The data represent mean ± SEM (*A*, *D*, *E*, *H*), **** $p < 0.0001$. EV, empty vector; IRF, interferon regulatory factor; MOI, multiplicity of infection; MHV, murine hepatitis virus; SeV, Sendai virus.

activation. IRF7-S1 is inactive in transcriptional activation due to lack of key phosphorylation sites (38). IRF7-S1, like IRF7-Wt, also interacted with NF-κB-p65 and suppressed inflammatory gene expression. Subsequently, IRF7-S1, when expressed in IRF7 KO or even in IRF3 KO cells, also efficiently suppressed inflammatory gene expression. We further evaluated whether the transcription-independent IRF7 function contributes to its antiviral responses. In myeloid and non-myeloid cells, ectopic expression of IRF7-S1 mutant efficiently suppressed MHV and SeV replication. Therefore, we uncovered a new functional branch of IRF7, independent of its transcriptional activity, to suppress cellular inflammatory responses and viral replication.

Viral infection rapidly activates IRF3, expressed ubiquitously, to trigger induction of IFNs and ISGs. IRF3 also functions independent of its IFN-inducing activity, triggering a direct pro-apoptotic pathway by interacting with BAX (9, 39–45), and an anti-inflammatory pathway by directly interacting with NF-κB-p65 (36, 37). As a result, IRF3-deficient cells and mice, lacking various functions of IRF3, exhibit enhanced viral replication and pathogenesis. IRF7, on the other hand, is expressed in restricted cell types, primarily in myeloid cells, and can also be induced by IFN signaling. IRF7, a master regulator of cellular IFN response and antiviral functions of the host, functions by inducing IFNs, primarily IFNα. Our results demonstrated IRF7 can also function independent of its transcriptional activity, a newly identified property of IRF7. Using nontranscriptional mutant IRF7-S1, we uncovered anti-inflammatory and antiviral activities of IRF7. Whether anti-inflammatory activity contributes to IRF7's antiviral activity is unclear; expressing IRF7-S1 in NF-κB–inactive cells and testing its antiviral activities will help reveal this. IRF7 exhibits robust antiviral activities against IAV and herpes simplex virus-1. Mutations associated with IRF7 gene led to HSV-1– and IAV-associated diseases in humans (24, 25, 46, 47). Recent studies also revealed IRF7 mutations are associated with COVID-19 severity (26, 27). These IRF7 functions likely depend on transcriptional induction of IFN; however, nontranscriptional function of IRF7 may also contribute to its overall antiviral responses. Future genetic screen may reveal whether mutations leading to nontranscriptional IRF7 may have protective responses. IRF7, in addition to antiviral

immunity, has functions in auto-immune diseases, for example, SLE, lupus (48, 49). These functions of IRF7 are also attributed from its ability to induce IFNα (50); however, future studies will reveal whether some of these functions are also controlled by its nontranscriptional activity.

Our results revealed IRF7, in addition to IRF3, has the property to interact with NF-κB to inhibit inflammatory gene expression. IRF7 interacted with NF-κB-p65 via a domain distinct from the IRF3-binding motif, suggesting IRFs may have evolved with ability to target NF-κB via multiple mechanisms. A similarity between IRF3 and IRF7 was identified in their inability to bind NF-κB-p50 subunit. Our results further added a complexity that IRF7 can compensate for IRF3 for cellular anti-inflammatory responses. These results may indicate that in the absence of IRF3 protein, which often happens during viral infection, IRF7 may help suppress cellular inflammation. However, because of cell-specific expression of IRF7, the anti-inflammatory responses may only be cell type–specific. IRF7 is either not expressed or expressed at a very low level but induced by virus infection and IFN signaling, suggesting the early part of cellular inflammatory responses may be controlled by IRF3, whereas the later phase, when IRF7 expression is further induced, may be controlled by IRF7. Our bioinformatic analyses followed by co-IP studies indicated that IRF5 also possesses NF-κB–binding motif and interacts with NF-κB-p65. Future studies will help reveal whether IRF5:NF-κB interaction has any functional implications or not. A previous study revealed anti-inflammatory function of IRF5 (51); however, whether such a function is mediated partially by targeting NF-κB needs to be investigated. Both IRF3 and IRF7 inhibit NF-κB signaling pathways by mechanisms in addition to targeting NF-κB-p65. In high-fat diet-induced liver disease model, IRF3 interacts with IKKβ, an upstream kinase that activates NF-κB, thereby suppressing NF-κB–dependent gene expression and liver injury (52). IRF7 also interacts with IKKβ, inhibiting inflammatory responses and cardiac hypertrophy (53). We also showed that in the liver injury model, IRF3 suppresses inflammatory gene expression by interacting with NF-κB-p65 (54). Therefore, IRFs have evolved with targeting different components of NF-κB signaling to efficiently suppress cellular inflammatory responses. Since NF-κB is a critical transcription factor involved in numerous cellular functions, its regulation by IRFs may form a basis for controlling various diseases, including sepsis, cancer etc, as well as normal cellular functions where NF-κB activity is involved.

Our studies with IRF3 and IRF7 underscore the nontranscriptional activities of these transcription factors. IRFs have been studied extensively for their ability to induce IFNs and IFN-related genes, mediated by their transcriptional activation. IRF3, IRF5, and IRF7 are critical IRFs, activated directly by virus infection, to regulate cellular antiviral responses (9, 30, 33, 55, 56). IRF1, on the other hand, is induced, cell type-specifically, and can also participate in cellular antiviral responses (57, 58). IRF9, a critical component of type-I IFN-signaling, participates in mounting antiviral responses and numerous other IFN-related functions (59). A deeper look at these IRFs for nontranscriptional activities will help reveal new cellular functions of these proteins with implications in many diseases. Use of nontranscriptional mutants of the IRFs will help uncover transcription-independent functions of these IRFs. STATs and p53, transcription factors involved in numerous cellular functions, have also been shown to act transcription-independently. STAT3 translocates to mitochondria to control cellular glycolysis (60, 61). P53, on the other hand, induces apoptotic cell death by transcription-independent activation, by translocating to mitochondria, interacting with and activating pro-apoptotic proteins (62, 63). Other transcription factors, for example, Oct1, and transcriptional co-activators, for example, β-catenin, Yap, which are primarily involved in cellular transcriptional responses, have been shown to have nontranscriptional roles (64–66). How a single protein performs multiple functions is a complex question and requires extensive genetic and biochemical investigation to answer. Our studies with IRF3 revealed differential activation mechanisms for different functional branches of IRF3 (36, 39–41, 67, 68). Knock-in mice expressing nontranscriptional mutants have been generated to evaluate relative contribution of transcriptional and nontranscriptional functions of these proteins. We engineered knock-in mice expressing a transcriptionally inactive mutant of IRF3 and demonstrated that such mice were able to protect against viral infection in the absence of transcriptional activities (40). Nontranscriptional functions of IRF3 have also been implicated in other diseases, including liver injury models (54, 69).

In summary, our study revealed a new function of IRF7, independent of its transcriptional activity, to inhibit NF-κB–dependent inflammatory genes and viral replication. Furthermore, IRF7 can compensate for IRF3 for cellular anti-inflammatory and antiviral responses. Future studies will reveal how the newly identified nontranscriptional function of IRF7 can function in other models beyond viral infection.

Experimental procedures

Antibodies

Antibodies used in this study were obtained as indicated: anti-Actin (Sigma-Aldrich #A5441); anti-TNFAIP3/A20 (Cell Signaling Technology [CST] #5630); anti-Flag (CST #2368 and Sigma-Aldrich #F1804); anti-HDAC1(CST #34589); anti-6X-His (Sigma-Aldrich: SAB2702219); anti-IRF3 (as described before (41)); anti-IFIT (as described before (41)); anti-IRF7 (CST# 39659); anti-phospho-IRF7 (CST# 24129); anti-Murine Coronavirus Nucleocapsid (N) protein (BEI Resources #NR-45106); anti-NF-κB p65 (CST# 8242S and Santa Cruz Biotechnology # sc-8008); anti-NF-κB phospho-p65 (CST# 3033S); antibody against Sendai virus C protein (as described before (67)), anti-V5 (CST #13202 and Thermo Fisher Scientific #R960-25).

Cell lines and viruses

Human cell lines HEK293T/17 (CRL-11268), HT1080 (CCL-121), and mouse cell lines RAW264.7 (TIB-71), L929 (CCL-1), NIH/3T3 (CRL-1658) were obtained from American

Type Culture Collection, mouse lung epithelium (Let1) cells (NR-42941), mouse macrophages WT and Irf7$^{-/-}$ cell lines (NR-9456, NR-15636) were obtained from BEI Resources. Cells were cultured in Dulbecco's modified Eagle's medium supplemented with 10% fetal bovine serum and 1% penicillin/streptomycin and maintained at 37 °C and under 5% CO_2. The cells are routinely treated with *mycoplasma* removal agent (MP Biomedicals). SeV Cantell was obtained from Charles Rivers Laboratories. Recombinant murine coronavirus strain icA59 (MHV-A59) was obtained from BEI (NR-43000) and grown in L929 cells according to manufacturer's information sheet. H1N1 IAV strain PR8 was kindly provided by Jacob Yount (OSU).

Cloning and mutant generation

Mouse IRF7 (Origene: NM_016850) was subcloned into pLVX-IRES-puromycin (Clontech) vector, which was subsequently used to construct His-tagged Wt mouse IRF7 and to generate V5-tagged deletion mutants. Deletion constructs of mouse IRF7 were generated by standard molecular cloning methods. Mouse IRF7 mutant S1 was generated from His-tagged Wt mouse IRF7 by overlap extension PCR and previously described procedures. All clones and mutants were verified by sequencing.

Cell lines with gene knockdown and overexpression

IRF7 expression was knocked down in RAW264.7 and Let1 cells by shRNA through lentivirus transduction. His-tagged and V5-tagged IRF7 plasmids were used to generate IRF7-overexpressed mouse Let1 and human HT1080 stable cell lines, respectively. Knockdown and overexpression of IRF7 levels were verified by qRT-PCR. IRF3 KO HT1080 or HEK293T cell lines were generated using CRISPR/Cas9 system, as described before (44).

Cell lysis and immunoblot

Harvested cells were lysed in 50 mM Tris buffer, pH 7.4 containing 150 mM of NaCl, 0.1% Triton X-100, 1 mM sodium orthovanadate, 10 mM of NaF, 10 mM of β-glycerophosphate, 5 mM sodium pyrophosphate, and protease/phosphatase inhibitors, followed by brief sonication and centrifugation for 30 min to clear the lysate. Total protein extracts were quantified using Bradford reagent (BIO-RAD #500–0006), and equal amounts of proteins were analyzed by SDS–PAGE, followed by immunoblot.

Co-immunoprecipitation

For co-IP, cells were lysed in EPPS buffer containing protease and phosphatase inhibitors (Roche). Cell lysates were subjected to repeated freeze-thaw cycles and were kept on ice for 20 min, followed by centrifugation to isolate the supernatants containing the proteins. Immunoprecipitation or pull-down reactions were performed using anti-V5 or Ni-NTA (for IRF7) and anti-Flag (for NF-κB-p65) agarose beads, using previously described procedures. For endogenous proteins, the cell lysates were incubated first with the primary antibodies followed by protein A/G agarose beads (SCBT# sc-2003). After overnight immunoprecipitation, beads were washed twice with EPPS buffer and once with radioimmunoprecipitation assay buffer. Bound proteins were boiled with SDS buffer containing 2-mercaptoethanol for 3 min to separate the proteins from the beads and were analyzed by SDS-PAGE, followed by immunoblot. Nuclear fractions of cells were isolated and analyzed using methods described before (40, 41).

Cell-free protein interaction assay

HEK293T cells expressing His-tagged IRF7 (His.IRF7) or Flag-tagged NF-κB-p65 (Flag.NF-κB-p65) were lysed separately in EPPS buffer containing protease inhibitors through repetitive freeze-thaw cycles; then proteins of interest were pull down by Ni-NTA agarose resin or immunoprecipitated with anti-Flag agarose beads overnight at 4 °C. Beads were washed with EPPS buffer containing 300 mM NaCl. His.IRF7 was eluted with imidazole and Flag.NF-κB-p65 was eluted with Flag peptide. The purified cell-free proteins were used for interaction assay, followed by analysis with SDS-PAGE.

Intracellular signaling activation and virus infection

TLR3 signaling was triggered by poly I:C addition (25 μg/ml) to the cell culture for 4 h before harvest. TLR4 signaling was stimulated by adding LPS (1 μg/ml) to the cell culture for 4 h. RLR signaling was triggered by transfecting cells with poly I:C using Lipofectamine 2000 (Thermo Fisher Scientific), indicating in the text as pIC+LF, for 2 h unless indicated otherwise. For virus infections, indicated cells were infected with either SeV (Cantell), IAV, or MHV at the multiplicity of infection of 5 in serum-free Dulbecco's modified Eagle's medium for 2 h, then the cells were washed with PBS and incubated in fresh normal growth medium. The infected cells were then harvested at the indicated time and subjected to analysis for cellular or viral gene expression using qRT-PCR or immunoblot, as described in the figure legends. For quantification of infectious MHV, supernatant from infected cells was collected and plaque assay was performed using L929 cells.

Protein alignment and visualization

Multiple sequence alignment of IRF proteins was performed using Clustal Omega, and 3D visualization was done with Visual Molecular Dynamics software. Visual Molecular Dynamics was developed with NIH support by the Theoretical and Computational Biophysics group at the Beckman Institute, University of Illinois at Urbana-Champaign (http://www.ks.uiuc.edu/).

Proximity ligation assay and confocal microscopy

Cells on coverslips were fixed using 4% paraformaldehyde (Electron Microscopy Sciences #15710). Cell membranes were permeabilized using 0.2% Triton X-100 (Thermo Fisher Scientific #9002–93-1). Cells were immuno-stained with anti-V5 and anti-Flag antibodies followed by duolink assay (DUO92008-3, DUO92004, DUO92002, Sigma-Aldrich)

according to the manufacturer's instructions. Coverslips were mounted with VectaShield/DAPI (H-1200, Vector Laboratories) on microscopy slides and analyzed using Olympus confocal microscope and Olympus Fluoview FV1000 software (https://www.olympus-lifescience.com/en/downloads/detail-iframe/?0[downloads][id]=847249651).

RNA isolation and qRT-PCR analyses

Total RNA was extracted with TRIzol (Sigma #T9424) and subjected to DNAse (Promega) treatment. DNAse-treated RNA was used to prepare complementary DNA using random hexamers and the ImProm-II Reverse Transcription Kit (Promega), according to the manufacturer's instructions. The complementary DNA was amplified using Radiant SYBR Green PCR mix (Alkali Scientific Inc.) in Roche LightCycler 96 instrument, and data were analyzed using LightCycler 480 Software, version 1.5 (https://lifescience.roche.com/global/en/products/product-category/lightcycler.html#4). The mRNA expression level for the genes of interest was normalized to that of 18S ribosomal RNA, and the normalized mRNA level was plotted using GraphPad Prism 9 software (www.graphpad.com). The primers used for qRT-PCR analyses are listed in Table S1.

Quantification and statistical analyses

Statistical analyses of qRT-PCR data were performed using GraphPad Prism 9 software. The qRT-PCR results shown are representative with technical replicates. p-values were calculated using two-tailed, unpaired Student's t-tests (when two groups were compared) or one-way ANOVA (when more than two groups were compared). $p < 0.05$ was considered statistically significant. Results presented are the representatives of at least three independent experiments.

Data availability

All data presented in this paper are contained within the manuscript.

Supporting information—This article contains supporting information.

Acknowledgments—We thank Travis Taylor, Kevin Pan, and Randall Worth for critical input on the study and Durga Sharma for technical support. The following reagents were obtained through BEI Resources, National Institute of Allergy and Infectious Diseases, NIH: anti-Murine Coronavirus Nucleocapsid (N) protein (NR-45106), mouse lung epithelium (Let1) cell line (NR-42941), mouse macrophage WT cell line (NR-9456), mouse macrophage Irf7−/− cell line (NR-15636), recombinant murine coronavirus strain icA59 (NR-43000).

Author contributions—S. F., S. P., R. C., and Sa. C. conceptualization; S. F., S. P., Su. C., R. C., and Sa. C. data curation; S. F., S. P., Su. C., R. C., and Sa. C. formal analysis; Sa. C. funding acquisition; S. F., S. P., Su. C., and Sa. C. investigation; S. F., S. P., R. C., and Sa. C. methodology; Sa. C. project administration; S. F., R. C., and Sa. C. writing–original draft; S. F., R. C., and Sa. C. writing–review and editing.

Funding and additional information—This work was supported in part by the National Institutes of Health grants AI155545 (Sa. C.), AI165521 (Sa. C.), AA027456 (Sa. C.), and Medical Research Society (Sa. C.), and the University of Toledo College of Medicine and Life Sciences startup funds (Sa. C. and R. C.). The content is solely the responsibility of the authors and does not necessarily represent the official views of the National Institutes of Health.

Conflict of interest—The authors declare that they have no conflicts of interest with the contents of this article.

Abbreviations—The abbreviations used are: co-IP, co-immunoprecipitation; CST, Cell Signaling Technology; IAV, Influenza A virus; IFN, interferon; IRF, interferon regulatory factor; ISG, IFN-stimulated gene; LPS, lipopolysaccharide; MHV, murine hepatitis virus; NT, non-targeting; PLA, proximity ligation assay; PRR, pathogen recognition receptor; SeV, Sendai virus; shIRF7, IRF7-shRNA; shNT, NT shRNA; TLR, toll-like receptor.

References

1. McNab, F., Mayer-Barber, K., Sher, A., Wack, A., and O'Garra, A. (2015) Type I interferons in infectious disease. *Nat. Rev. Immunol.* **15**, 87–103
2. Mesev, E. V., LeDesma, R. A., and Ploss, A. (2019) Decoding type I and III interferon signalling during viral infection. *Nat. Microbiol.* **4**, 914–924
3. Fensterl, V., and Sen, G. C. (2009) Interferons and viral infections. *Biofactors* **35**, 14–20
4. Schoggins, J. W. (2019) Interferon-stimulated genes: what do they all do? *Annu. Rev. Virol.* **6**, 567–584
5. Fensterl, V., Chattopadhyay, S., and Sen, G. C. (2015) No love lost between viruses and interferons. *Annu. Rev. Virol.* **2**, 549–572
6. Ivashkiv, L. B., and Donlin, L. T. (2014) Regulation of type I interferon responses. *Nat. Rev. Immunol.* **14**, 36–49
7. Chattopadhyay, S., and Sen, G. C. (2014) Tyrosine phosphorylation in Toll-like receptor signaling. *Cytokine Growth Factor Rev.* **25**, 533–541
8. Bruns, A. M., and Horvath, C. M. (2014) Antiviral RNA recognition and assembly by RLR family innate immune sensors. *Cytokine Growth Factor Rev.* **25**, 507–512
9. Glanz, A., Chakravarty, S., Varghese, M., Kottapalli, A., Fan, S., Chakravarti, R., *et al.* (2021) Transcriptional and non-transcriptional activation, posttranslational modifications, and antiviral functions of interferon regulatory factor 3 and viral antagonism by the SARS-coronavirus. *Viruses* **13**, 575
10. Chen, K., Liu, J., and Cao, X. (2017) Regulation of type I interferon signaling in immunity and inflammation: a comprehensive review. *J. Autoimmun.* **83**, 1–11
11. Chakravarty, S., Subramanian, G., Popli, S., Veleeparambil, M., Fan, S., Chakravarti, R., *et al.* (2023) Interferon-stimulated gene TDRD7 interacts with AMPK and inhibits its activation to suppress viral replication and pathogenesis. *mBio* **14**, e0061123
12. Subramanian, G., Kuzmanovic, T., Zhang, Y., Peter, C. B., Veleeparambil, M., Chakravarti, R., *et al.* (2018) A new mechanism of interferon's antiviral action: induction of autophagy, essential for paramyxovirus replication, is inhibited by the interferon stimulated gene, TDRD7. *PLoS Pathog.* **14**, e1006877
13. Faist, A., Janowski, J., Kumar, S., Hinse, S., Caliskan, D. M., Lange, J., *et al.* (2022) Virus infection and systemic inflammation: lessons learnt from COVID-19 and beyond. *Cells* **11**, 2198
14. Sandstrom, T. S., Ranganath, N., and Angel, J. B. (2017) Impairment of the type I interferon response by HIV-1: potential targets for HIV eradication. *Cytokine Growth Factor Rev.* **37**, 1–16
15. Mitchell, S., Vargas, J., and Hoffmann, A. (2016) Signaling via the NFkappaB system. *Wiley Interdiscip. Rev. Syst. Biol. Med.* **8**, 227–241

16. Hayden, M. S., and Ghosh, S. (2004) Signaling to NF-kappaB. *Genes Dev.* **18**, 2195–2224
17. Zhao, J., He, S., Minassian, A., Li, J., and Feng, P. (2015) Recent advances on viral manipulation of NF-kappaB signaling pathway. *Curr. Opin. Virol.* **15**, 103–111
18. Hancock, M. H., and Nelson, J. A. (2017) Modulation of the NFkappab signalling pathway by human cytomegalovirus. *Virology (Hyderabad)* **1**, 104
19. Tavares, L. P., Teixeira, M. M., and Garcia, C. C. (2017) The inflammatory response triggered by Influenza virus: a two edged sword. *Inflamm. Res.* **66**, 283–302
20. Jochems, S. P., Marcon, F., Carniel, B. F., Holloway, M., Mitsi, E., Smith, E., *et al.* (2018) Inflammation induced by influenza virus impairs human innate immune control of pneumococcus. *Nat. Immunol.* **19**, 1299–1308
21. Attiq, A., Yao, L. J., Afzal, S., and Khan, M. A. (2021) The triumvirate of NF-kappaB, inflammation and cytokine storm in COVID-19. *Int. Immunopharmacol.* **101**, 108255
22. Honda, K., Yanai, H., Negishi, H., Asagiri, M., Sato, M., Mizutani, T., *et al.* (2005) IRF-7 is the master regulator of type-I interferon-dependent immune responses. *Nature* **434**, 772–777
23. Ning, S., Pagano, J. S., and Barber, G. N. (2011) IRF7: activation, regulation, modification and function. *Genes Immun.* **12**, 399–414
24. Ciancanelli, M. J., Huang, S. X., Luthra, P., Garner, H., Itan, Y., Volpi, S., *et al.* (2015) Infectious disease. Life-threatening influenza and impaired interferon amplification in human IRF7 deficiency. *Science* **348**, 448–453
25. Thomsen, M. M., Jorgensen, S. E., Gad, H. H., Storgaard, M., Gjedsted, J., Christiansen, M., *et al.* (2019) Defective interferon priming and impaired antiviral responses in a patient with an IRF7 variant and severe influenza. *Med. Microbiol. Immunol.* **208**, 869–876
26. Zhang, Q., Bastard, P., Liu, Z., Le Pen, J., Moncada-Velez, M., Chen, J., *et al.* (2020) Inborn errors of type I IFN immunity in patients with life-threatening COVID-19. *Science* **370**, eabd4570
27. Zhang, Q., Matuozzo, D., Le Pen, J., Lee, D., Moens, L., Asano, T., *et al.* (2022) Recessive inborn errors of type I IFN immunity in children with COVID-19 pneumonia. *J. Exp. Med.* **219**, e20220131
28. Lazear, H. M., Lancaster, A., Wilkins, C., Suthar, M. S., Huang, A., Vick, S. C., *et al.* (2013) IRF-3, IRF-5, and IRF-7 coordinately regulate the type I IFN response in myeloid dendritic cells downstream of MAVS signaling. *PLoS Pathog.* **9**, e1003118
29. Wu, W., Zhang, W., Tian, L., Brown, B. R., Walters, M. S., and Metcalf, J. P. (2020) IRF7 is required for the second phase interferon induction during influenza virus infection in human lung epithelia. *Viruses* **12**, 377
30. Barnes, B. J., Richards, J., Mancl, M., Hanash, S., Beretta, L., and Pitha, P. M. (2004) Global and distinct targets of IRF-5 and IRF-7 during innate response to viral infection. *J. Biol. Chem.* **279**, 45194–45207
31. Kusiak, A., and Brady, G. (2022) Bifurcation of signalling in human innate immune pathways to NF-kB and IRF family activation. *Biochem. Pharmacol.* **205**, 115246
32. Iwanaszko, M., and Kimmel, M. (2015) NF-kappaB and IRF pathways: cross-regulation on target genes promoter level. *BMC Genomics* **16**, 307
33. Jefferies, C. A. (2019) Regulating IRFs in IFN driven disease. *Front. Immunol.* **10**, 325
34. Czerkies, M., Korwek, Z., Prus, W., Kochanczyk, M., Jaruszewicz-Blonska, J., Tudelska, K., *et al.* (2018) Cell fate in antiviral response arises in the crosstalk of IRF, NF-kappaB and JAK/STAT pathways. *Nat. Commun.* **9**, 493
35. Tian, B., Yang, J., Zhao, Y., Ivanciuc, T., Sun, H., Garofalo, R. P., *et al.* (2017) BRD4 couples NF-kappaB/RelA with airway inflammation and the IRF-RIG-I amplification loop in respiratory syncytial virus infection. *J. Virol.* **91**, e00007-17
36. Popli, S., Chakravarty, S., Fan, S., Glanz, A., Aras, S., Nagy, L. E., *et al.* (2022) IRF3 inhibits nuclear translocation of NF-kappaB to prevent viral inflammation. *Proc. Natl. Acad. Sci. U. S. A.* **119**, e2121385119
37. Chakravarty, S., Chakravarti, R., and Chattopadhyay, S. (2023) Inflammatory control of viral infection. *Viruses* **15**, 1579
38. Caillaud, A., Hovanessian, A. G., Levy, D. E., and Marie, I. J. (2005) Regulatory serine residues mediate phosphorylation-dependent and phosphorylation-independent activation of interferon regulatory factor 7. *J. Biol. Chem.* **280**, 17671–17677
39. Chattopadhyay, S., Fensterl, V., Zhang, Y., Veleeparambil, M., Yamashita, M., and Sen, G. C. (2013) Role of interferon regulatory factor 3-mediated apoptosis in the establishment and maintenance of persistent infection by Sendai virus. *J. Virol.* **87**, 16–24
40. Chattopadhyay, S., Kuzmanovic, T., Zhang, Y., Wetzel, J. L., and Sen, G. C. (2016) Ubiquitination of the transcription factor IRF-3 activates RIPA, the apoptotic pathway that protects mice from viral pathogenesis. *Immunity* **44**, 1151–1161
41. Chattopadhyay, S., Marques, J. T., Yamashita, M., Peters, K. L., Smith, K., Desai, A., *et al.* (2010) Viral apoptosis is induced by IRF-3-mediated activation of Bax. *EMBO J.* **29**, 1762–1773
42. Chattopadhyay, S., and Sen, G. C. (2010) IRF-3 and Bax: a deadly affair. *Cell Cycle* **9**, 2479–2480
43. Glanz, A., Chakravarty, S., Fan, S., Chawla, K., Subramanian, G., Rahman, T., *et al.* (2021) Autophagic degradation of IRF3 induced by the small-molecule auranofin inhibits its transcriptional and proapoptotic activities. *J. Biol. Chem.* **297**, 101274
44. Glanz, A., Chawla, K., Fabry, S., Subramanian, G., Garcia, J., Jay, B., *et al.* (2020) High throughput screening of FDA-approved drug library reveals the compounds that promote IRF3-mediated pro-apoptotic pathway inhibit virus replication. *Viruses* **12**, 442
45. White, C. L., Chattopadhyay, S., and Sen, G. C. (2011) Phosphatidylinositol 3-kinase signaling delays sendai virus-induced apoptosis by preventing XIAP degradation. *J. Virol.* **85**, 5224–5227
46. Irving, A. T., Zhang, Q., Kong, P. S., Luko, K., Rozario, P., Wen, M., *et al.* (2020) Interferon regulatory factors IRF1 and IRF7 directly regulate gene expression in bats in response to viral infection. *Cell Rep.* **33**, 108345
47. Tucker, M. H., Yu, W., Menden, H., Xia, S., Schreck, C. F., Gibson, M., *et al.* (2023) IRF7 and UNC93B1 variants in an infant with recurrent herpes simplex virus infection. *J. Clin. Invest.* **133**, e154016
48. Xu, W. D., Zhang, Y. J., Xu, K., Zhai, Y., Li, B. Z., Pan, H. F., *et al.* (2012) IRF7, a functional factor associates with systemic lupus erythematosus. *Cytokine* **58**, 317–320
49. Fu, Q., Zhao, J., Qian, X., Wong, J. L., Kaufman, K. M., Yu, C. Y., *et al.* (2011) Association of a functional IRF7 variant with systemic lupus erythematosus. *Arthritis Rheum.* **63**, 749–754
50. Jensen, M. A., and Niewold, T. B. (2015) Interferon regulatory factors: critical mediators of human lupus. *Transl. Res.* **165**, 283–295
51. Weiss, M., Byrne, A. J., Blazek, K., Saliba, D. G., Pease, J. E., Perocheau, D., *et al.* (2015) IRF5 controls both acute and chronic inflammation. *Proc. Natl. Acad. Sci. U. S. A.* **112**, 11001–11006
52. Wang, X. A., Zhang, R., She, Z. G., Zhang, X. F., Jiang, D. S., Wang, T., *et al.* (2014) Interferon regulatory factor 3 constrains IKKbeta/NF-kappaB signaling to alleviate hepatic steatosis and insulin resistance. *Hepatology* **59**, 870–885
53. Jiang, D. S., Liu, Y., Zhou, H., Zhang, Y., Zhang, X. D., Zhang, X. F., *et al.* (2014) Interferon regulatory factor 7 functions as a novel negative regulator of pathological cardiac hypertrophy. *Hypertension* **63**, 713–722
54. Sanz-Garcia, C., McMullen, M. R., Chattopadhyay, S., Roychowdhury, S., Sen, G., and Nagy, L. E. (2019) Nontranscriptional activity of interferon regulatory factor 3 protects mice from high-fat diet-induced liver injury. *Hepatol. Commun.* **3**, 1626–1641
55. Hiscott, J. (2007) Triggering the innate antiviral response through IRF-3 activation. *J. Biol. Chem.* **282**, 15325–15329
56. Yanai, H., Chen, H. M., Inuzuka, T., Kondo, S., Mak, T. W., Takaoka, A., *et al.* (2007) Role of IFN regulatory factor 5 transcription factor in antiviral immunity and tumor suppression. *Proc. Natl. Acad. Sci. U. S. A.* **104**, 3402–3407
57. Panda, D., Gjinaj, E., Bachu, M., Squire, E., Novatt, H., Ozato, K., *et al.* (2019) IRF1 maintains optimal constitutive expression of antiviral genes and regulates the early antiviral response. *Front. Immunol.* **10**, 1019
58. Mboko, W. P., Mounce, B. C., Emmer, J., Darrah, E., Patel, S. B., and Tarakanova, V. L. (2014) Interferon regulatory factor 1 restricts gammaherpesvirus replication in primary immune cells. *J. Virol.* **88**, 6993–7004

59. Suprunenko, T., and Hofer, M. J. (2016) The emerging role of interferon regulatory factor 9 in the antiviral host response and beyond. *Cytokine Growth Factor Rev.* **29**, 35–43
60. Camporeale, A., Demaria, M., Monteleone, E., Giorgi, C., Wieckowski, M. R., Pinton, P., *et al.* (2014) STAT3 activities and energy metabolism: dangerous liaisons. *Cancers (Basel)* **6**, 1579–1596
61. Xu, Y. S., Liang, J. J., Wang, Y., Zhao, X. J., Xu, L., Xu, Y. Y., *et al.* (2016) STAT3 undergoes acetylation-dependent mitochondrial translocation to regulate pyruvate metabolism. *Sci. Rep.* **6**, 39517
62. Vaseva, A. V., and Moll, U. M. (2009) The mitochondrial p53 pathway. *Biochim. Biophys. Acta* **1787**, 414–420
63. Castrogiovanni, C., Waterschoot, B., De Backer, O., and Dumont, P. (2018) Serine 392 phosphorylation modulates p53 mitochondrial translocation and transcription-independent apoptosis. *Cell Death Differ.* **25**, 190–203
64. Bui, D. A., Lee, W., White, A. E., Harper, J. W., Schackmann, R. C., Overholtzer, M., *et al.* (2016) Cytokinesis involves a nontranscriptional function of the Hippo pathway effector YAP. *Sci. Signal.* **9**, ra23
65. Kim, H., Wu, J., Ye, S., Tai, C. I., Zhou, X., Yan, H., *et al.* (2013) Modulation of beta-catenin function maintains mouse epiblast stem cell and human embryonic stem cell self-renewal. *Nat. Commun.* **4**, 2403
66. Ding, Y., Su, S., Tang, W., Zhang, X., Chen, S., Zhu, G., *et al.* (2014) Enrichment of the β-catenin-TCF complex at the S and G2 phases ensures cell survival and cell cycle progression. *J. Cell Sci.* **127**, 4833–4845
67. Chattopadhyay, S., Yamashita, M., Zhang, Y., and Sen, G. C. (2011) The IRF-3/Bax-mediated apoptotic pathway, activated by viral cytoplasmic RNA and DNA, inhibits virus replication. *J. Virol.* **85**, 3708–3716
68. Chattopadhyay, S., and Sen, G. C. (2017) RIG-I-like receptor-induced IRF3 mediated pathway of apoptosis (RIPA): a new antiviral pathway. *Protein Cell* **8**, 165–168
69. Sanz-Garcia, C., Poulsen, K. L., Bellos, D., Wang, H., McMullen, M. R., Li, X., *et al.* (2019) The non-transcriptional activity of IRF3 modulates hepatic immune cell populations in acute-on-chronic ethanol administration in mice. *J. Hepatol.* **70**, 974–984